FORMULATING AND OPTIMIZING THE RHEOLOGICAL PROPERTIES OF A COMPOSITE BONE CEMENT USING MIXTURE DESIGN

Océane Ly[1,2], Francine Monchau[1], Sébastien Rémond[2], Christine Lors[2], Alain Jouanneaux[3], Étienne Debarre[1], Denis Damidot[2]

[1]Laboratoire Génie Civil et géo-Environnement EA 4515, Pôle Béthune, Université d'Artois, 1230 rue de l'Université, 62440 Béthune, France

[2]IMT Lille Douai, Univ. Lille, EA 4515 – LGCgE – Laboratoire de Génie Civil et géo-Environnement, Département Génie Civil & Environnemental, 941 rue Charles-Bourseul, 59508 Douai, France

[3]Institut des Molécules et des Matériaux du Mans (IMMM), UMR-CNRS n° 6283, Université du Maine, avenue O. Messiaen, 72085 Le Mans, France

Abstract

The aim of our study was to optimize the formulation of the powder content of a bone cement based on an acrylic hydrogel, 2-hydroxyethyl methacrylate (HEMA), in order to obtain satisfactory rheological properties. A bone cement containing HEMA as a liquid phase (40% wt) and a blend of corn starch, cellulose acetate and a ceramic filler (alumina) in variable proportions as a solid phase (60% wt) was investigated by means of a mixture design. Each cement formulation was characterized using the complex shear modulus G related to the rheological behaviour. The mixture design strategy was applied and three application-targeted formulations resembling three commercial cements rheology were determined.*

Key words: *composite bone cement, experimental design, rheology, complex shear modulus*

1. INTRODUCTION

Biomaterials, and especially bone cements, have a wide range of applications in orthopaedic and maxillofacial surgeries and dentistry (Dorozhkin2010, Eliaz&Metoki 2017). Particularly, calcium phosphate and composite cements are known for their excellent bioactivity, good osteoconductivity and biocompatibility. They are therefore used in medical applications for bone regeneration (Bohner 2000; Combes et al. 2010).

Currently, bone cements can be used in the form of a dough in order to fill in bone defects or as a glue between bone and prosthesis for anchorage in dental surgery and arthroplasty (Chaudhry & Dunlop 2012), or in the form of a paste directly injected into a bone site as a minimally invasive treatment in percutaneous vertebroplasty (Buchbinder et al. 2015), in difficult-to-reach small cavities for practical reasons or as a filling after tooth devitalization. Nowadays, the potential of these cements is clearly stated and several studies aimed to optimize their setting time and temperature *in situ*, their mechanical properties or their form and aspect for handling issues (Guo et al. 2005; Saha & Pal 1984; Marrs et al. 2006).

While the majority of commercially available bone cements are either calcium phosphate cements or poly(methyl methacrylate) (PMMA) cements, in recent years, special attention has been paid to the production of a new class of cement based on hydrogels. Traditional cements, and especially PMMA-based ones, while widely used, have some drawbacks that need to be addressed. Among these, a retraction of the cement inside the bone site can be observed after implantation into the living body (Lewis 1997). This can be particularly inconvenient as it diminishes the efficiency of the treatment of the bone defect or loosens the adhesion between bone and prosthesis. To minimize this risk of retraction, a hydrogel can be used as a base instead of PMMA.

A hydrogel is a hydrophilic molecule which is commonly used in contact lenses or in biomedical engineering as cell and drug delivery systems. Its hydrophilicity makes it capable of absorbing the water of the medium and of swelling consequently. Thus, a hydrogel is a perfect candidate polymer to

avoid the shrinkage and underfilling of the bone defect cavity. Previous attempts have been made using acrylic acid (Greenberg &Kamel 1976; Boesel, Mano & Reis 2004) and then poly(hydroxyethyl methacrylate) (pHEMA) (Boesel & Reis 2004) hydrogels. One used a system composed of HEMA as a liquid phase and a blend of starch, cellulose acetate and bioglass (Boesel & Reis 2004).

However, a huge number of formulations are possible and the proportions of each component must be determined in order to achieve the best compromise in properties. In addition, there is a lack of information about the influence of each component on the final properties of the cement. In fact, varying quantities of each component leads to the modification of the properties of the mixture. For example, a high quantity of water in a solid/liquid mixture gives a very liquid paste. At last, the appropriate formulation of the cement is often found using a trial and error approach.

Instead of applying this classical experimental approach, we used in this study a statistical design of experiments (DoE), more precisely a mixture design (Eriksson et al. 2008), which will allow us, from a minimum number of well-chosen experimental runs, to model each ingredient effect on the ease of handling of a hydrogel-based cement according to its use.

The aim of this study was to obtain a formulation with adequate properties to its application by varying the amount of each component. For this, we chose to focus on the rheological behaviour of the formulations. Rheology is the study of deformation and flow of a material under an applied stress. It is particularly appropriate for studies concerning processability of materials as an end use. To a given application of a cement corresponds a rheological property (e.g. viscosity) which shall be high for a use as a paste, and low for an injectable material.

The objective of our work was to obtain from the DoE a reliable mathematical model connecting ingredient amounts and final properties in order to i) determine the required amount of each powder component of the cement yielding specific rheological characteristics and ii) develop three formulations with different rheological properties to adapt to different medical applications. Our approach led to try and imitate the rheological behaviour of three commonly used commercial bone cements, Palacos R, Simplex P and Zimmer Low Viscosity Cement (LVC) by applying the mathematical model to cements made of HEMA, starch, cellulose acetate and a bioceramic.

2. MATERIALS AND METHODS

2.1. Cement preparation

The cement paste was composed of two phases, one solid and one liquid, which were mixed thoroughly by hand in a silicon rubber mould with a metal spatula for 30 s.

The solid phase consisted of a blend of corn starch (Unilever France, France), cellulose acetate (Acros Organics, USA) and bioceramic (alumina) powders (Almatis GmbH, Germany) in varying proportions.

The liquid phase consisted of HEMA (stabilised, 97%, Acros Organics, USA), the acrylic monomer.

As far as we know, the blend of corn starch/cellulose acetate in bone cements was first investigated by Pereira et al. (1998) and was aimed to provide mechanical support to the defect as well as bone regeneration while the cement degraded progressively afterwards. Alumina was used as a bioceramic for a polymer-ceramic composite dental bone cement by Greenberg &Kamel (1976). HEMA was used as a moderately hydrophilic matrix by Boesel & Reis (2004).

For all the formulations, the mass solid-to-liquid ratio (S/L) was kept constant at 60/40 for the cement paste to keep a workable consistency.

These cements were prepared using commercial powders without further treatment. Their characteristics were determined according to the methods mentioned in Section 2.2.

2.2. Powders characterization

Dry phase diffraction granulometry was performed on the powders in order to measure their median particle size (D50) according to Fraunhofer model with an LS particle size analyser (LS 13 320, Beckman Coulter, CA, USA).Specific surface area of the powders was obtained by N_2 absorption and the Brunauer-Emmett-Teller (BET) method (Autopore IV 9505, Micromeritics, GA, USA). Density of the particles was measured by helium pycnometry (AccuPyc 1330, Micromeritics, GA, USA).

Alumina powder was analysed by X-ray powder diffraction (XRD) using Co Kα radiation at 35 kV and 40 mA and with a 2θ range of 6°-84°. The phase identification was made by the XRD phase identification software Diffrac.Eva V3.1.

2.3. Determination of the rheological properties of the samples

2.3.1. Basic principles of rheology and oscillatory rheometry

Basically, viscosity is the property of a material which is the most used to describe its behaviour towards flow. It corresponds to the ratio of shear stress to shear rate of that material at fixed temperature and pressure and is represented by flow curves plotting the shear stress (τ) with respect to the shear rate ($\dot{\gamma}$). For Newtonian fluids like water, the viscosity is constant whatever the shear rate. In this case, the viscosity η is defined by Equation 1.

$\tau = \eta\dot{\gamma}$ (Eq. 1)

However, most polymers are not Newtonian, meaning that their viscosity is not a constant and varies with the shear rate. Instead, they are viscoelastic, meaning that their properties change between viscous fluid-like and elastic solid-like. Bone cements fall into this category of materials, and especially ours which is based on a polymer, poly(hydroxyethyl methacrylate).

These viscoelastic properties are particularly relevant when studying the behaviour of the mixtures under a stress, which is the case when a cement is processed after mixing by being injected with an injection gun for example.

Viscosity is measured by means of devices such as viscometers or rheometers. While viscometers allow for the measurement of viscosity only, rheometers have the ability of measuring other parameters which describe better the viscoelastic properties of the material when applying an oscillatory shear. Amongst these properties, we can cite G', G", G*, tan(δ) and η* which will be explained later. To understand them, we need to take a look at how a rheometer works.

When an oscillatory shear is applied by the rheometer on the sample, the sample responds to the stress (τ) by a corresponding strain (γ) of given amplitude. Expressions of stress and strain are given in Equations 2 and 3 respectively. However, this response is out of phase with respect to the stress. This phase shift or phase angle (δ) (also called loss angle) is thus measured and its tangent tan(δ) indicates the material damping or loss factor. For comparison, δ equals zero for an elastic solid, π/2 for a viscous fluid and lies between zero and π/2 for a viscoelastic material.

$\tau(t) = \tau_0 \sin(\omega t + \delta)$ (Eq. 2)

$\gamma(t) = \gamma_0 \sin(\omega t)$ (Eq. 3)

Tan(δ) shows the dominance of either a solid-like behaviour – represented by G', the elastic modulus or storage modulus, which corresponds to the energy accumulated by the sample upon stress – or a liquid-like behaviour – represented by G", the viscous modulus or loss modulus, which corresponds to the energy dissipated after stress – of the sample (Eq. 4, 5, 6).

$\tan(\delta) = \frac{G"}{G'}$ (Eq. 4)

$G' = \frac{\tau_0}{\gamma_0}\cos(\delta)$ (Eq. 5)

$G" = \frac{\tau_0}{\gamma_0}\sin(\delta)$ (Eq. 6)

G* characterizes the overall resistance of the sample to strain and has two components, G' and G". These three parameters are linked according to Equations 7 and 8 (where *i* is the imaginary unit), G* thus summarizing the viscoelastic behaviour of the samples.

$|G^*| = \sqrt{G'^2 + G''^2}$ (Eq. 7)

$G^* = G' + iG''$ (Eq. 8)

Exhaustive details about these rheological parameters can be found elsewhere (Aho et al. 2015; Farrar & Rose 2001).

2.3.2. Rheological measurements

In this study, the rheological properties are represented by the measurement of the complex shear modulus |G*|.

The rheological properties of the samples were assessed at a controlled room temperature of 20 °C, in operating chamber conditions, using a table-top rotational rheometer (MCR102, Anton Paar, Austria). In these tests, a parallel-plate configuration was used, with one top rotating plate and one bottom static plate. Both had a diameter of 25 mm. This kind of geometry is particularly convenient for our material as it allows the study of small volumes of material with large particles, with a large range of viscosity. This measurement of the rheological properties was performed in dynamic oscillation mode, with a constant oscillatory shear of 1%, at a frequency of 1 Hz.

After the 30-second homogenisation of the solid and the liquid phases, the resulting cement paste was deposited onto the bottom plate of the rheometer with a spatula, before the top plate was put to contact with the paste sample until a 1.5-mm gap between both plates was reached. The wideness of the gap is commonly chosen to be at least ten times the size of the largest particles of the blend (Van Wazer et al. 1963) (Section 3.1, Table 4). However, in order to avoid the possible leakage of the most liquid formulations off the bottom plate, it was reduced to that size. Excess material was trimmed with a metal spatula and the oscillation of the upper plate began 2 min after the beginning of the mixing.

G* was measured 7 min after the beginning of the mixing. This delay corresponded to an estimation of the time needed to prepare the mix and to put it into a syringe in a comfortable way before injection.

For a better understanding of the rheological behaviour of the mixtures, a mixture design approach was used as described in Section 2.4.

2.3.3. Targeted rheological characteristics

From the study of the literature (Farrar & Rose 2001), three commercial cements (Palacos R, Simplex P and Zimmer Low Viscosity Cement (LVC)) were chosen for their very different rheological characteristics. Indeed, Palacos R is mainly used as a paste to fill in bone defects, whereas Zimmer LVC is an injectable cement. Intermediate between these two forms is Simplex P. Their measured G* is indicated in Table 1. It is noteworthy that in Farrar & Rose's work (2001), the measurements began between 60 and 100 s after the beginning of mixing of the two phases of each cement. A time of measurement at 7 min after the beginning of mixing thus corresponds to 320 or 360 s (Table 1). In order to run our model, we calculated the mean G* value of both times and based the computing of our formulations on it.

Table 1. Experimental values of G* at 7 min for three commercial bone cements (from Farrar & Rose 2001)

	Palacos R (Pa)	**Simplex P (Pa)**	**Zimmer LVC (Pa)**
G* at 320 s (Pa)	53,110	30,950	610
G* at 360 s (Pa)	60,940	35,360	840
Mean G*	57,025	33,155	725

A DoE model, described in Section 2.4.was developed and aimed at being reliable to adjust the G* of the final composition according to the surgeon's needs.

2.4. Mixture design

2.4.1. Introduction to mixture design

Briefly, a blending process in which all ingredients – called mixture factors – sum to 100% can be efficiently investigated by using a mixture design for changing composition and exploring how such changes will affect the chosen responses characteristics of the mixture behaviour. In this study the considered response (Y_{G*}) was the complex shear modulus (G*) at 7 min which represents the resistance of the material to strain. Our objective was to attain a target value of G* with a formulation whose amount of bioceramic is as high as possible in order to promote the biological properties (osteoconduction and osteoblastic activity) of the cement.

2.4.2. Mixture factors and experimental domain

In this study, three mixture factors are considered and all of them are solely part of the solid phase. They are defined as the weight proportion of bioceramic (X_1), corn starch (X_2) and cellulose acetate (X_3).

For a three-ingredient mixture, the experimental domain is an equilateral triangle when all proportions can vary from 0 to 1. On the basis of preliminary experimental results, we chose to reduce this domain to an irregular polygon in order to keep a workable consistency of the paste (Fig. 1). Selected lower and upper bounds are given in Table 2.

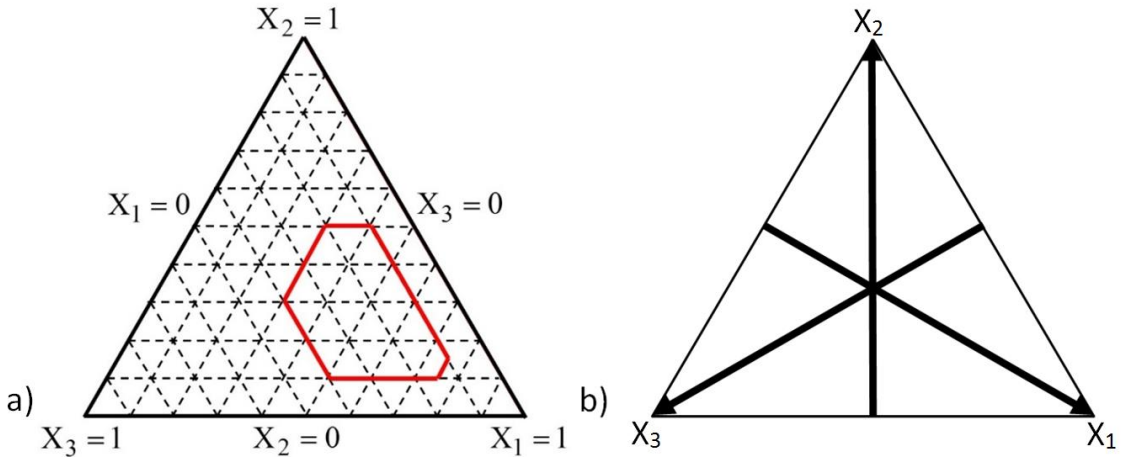


Fig. 1. Studied experimental domain. Fig. 1 a) shows the studied restricted domain bounded by the bold red line inside the general domain; Fig. 1 b) specifies the variations of X_1, X_2 and X_3 along the triangle.

Table 2. Investigated mixture factors of the bone cement and their limit bounds.

Factor	**Bioceramic (X_1)**	**Starch (X_2)**	**Cellulose acetate (X_3)**
Lower bound	0.3	0.1	0.1
Upper bound	0.75	0.5	0.4

2.4.3. Mixture model and generation of the mixture design

Positioning the experimental points within the experimental domain is of crucial importance to obtain a reliable and accurate mathematical model connecting response Y_{G*} and mixture factors Xi. As optimization is required in this study, the response was modelled with a quadratic regression model given by the following equation (Eq. 9):

$$\hat{Y} = \beta_0 + \sum_{i=1}^{q} \beta_i X_i + \sum_{i=1}^{q} \beta_{ii} X_i^2 + \sum_{i=1}^{q} \sum_{i<j}^{q} \beta_{ij} X_i X_j \quad \text{(Eq. 9)}$$

with the overall external constraint $X_1 + X_2 + X_3 = 1$, and where β are the model coefficients and X_k are the fractions of the three mixture ingredients expressed in the range defined in Table 2 above.

In presence of an irregular experimental domain, the mixture design must be computer generated. The specific DoE software MODDE 8.0 (Umetrics, Sweden) was used to build the design, and then to carry out mathematical, graphical and statistical analysis of the collected data.

Selecting the D-optimal specific option implemented in MODDE yielded a satisfactory solution including 8 runs which ensure a homogeneous coverage of the experimental domain. These designed runs labelled from 1 to 8 are shown in Figure 2 with their compositions in Table 3. For optimization purpose, it was relevant to add extra points No. 9 and 10 situated within the experimental region. Experiments No. 1 to 3 and 11 correspond to preliminary test runs. They were measured only once as well as points No. 9 and 10, whereas experiments No. 4 to 8 which are well spread throughout the experimental domain were measured three times. These replicated experiments will enable the Lack-Of-Fit test to be achieved, as mentioned below. A total of 21 runs was thus performed in the study.

Table 3. Experimental compositions.

Formulation number	Bioceramic (X_1)	Starch (X_2)	Cellulose acetate (X_3)
1	0.75	0.125	0.125
2	0.333	0.5	0.167
3	0.4	0.2	0.4
4	0.5	0.25	0.25
5	0.6	0.3	0.1
6	0.3	0.4	0.3
7	0.6	0.1	0.3
8	0.45	0.45	0.1
9	0.41	0.37	0.22
10	0.63	0.185	0.185
11	0.55	0.27	0.18

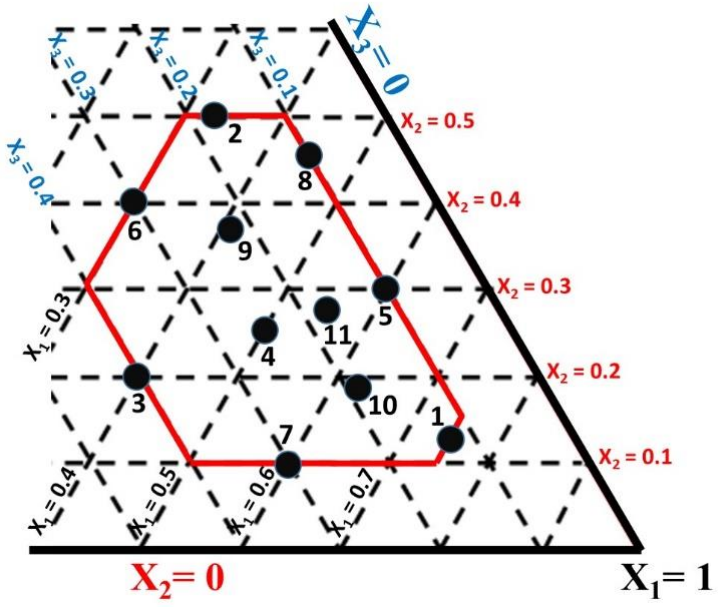


Fig. 2. Spatial representation of the studied domain.

2.4.4. Coefficient and model evaluation

The model coefficients were determined using the partial least squares (PLS) regression method (Wold et al. 1984; Kettaneh-Wold 1992) and coefficients with a p-value less than 0.05 were considered significant with 95% confidence. The model was evaluated using different tools: 1) the goodness of fit R^2 and goodness of prediction Q^2 statistics, 2) the analysis of variance which is useful for checking the adequacy of a regression model in terms of Lack-Of-Fit test and 3) the normal probability plot of residuals for verifying the normal distribution of residuals and for detecting deviating experiments.

3. RESULTS AND DISCUSSION

3.1. Powders characterization

The D50 particle size, BET surface area and density values of the three powders are presented in Table 4. With the particle size, we were able to determine the gap between the two plates of the rheometer by multiplying the highest D50 value – 218.00 µm, that of cellulose acetate particles so far – by ten, giving a 2-mm-wide gap. However, it was lessened to 1.5 mm to prevent leakage of the most liquid pastes, as explained in Section 2.3.2. The smallest particles are those of alumina (1.09 µm), and starch particles follow with a tenfold-bigger size (13.97 µm). For the specific surface area, cellulose acetate once more shows the highest value of 6.73 m^2/g, followed by alumina (1.64 m^2/g) which showed the smallest particle distribution but also the highest density (3.96). Apparent densities measured by helium pycnometry were more or less similar to values given in the literature: 3.96 against 3.4 to 4.0 (Lewis 2007, p.49) for alumina, 1.37 against 1.27 to 1.34 for cellulose acetate (Lewis 1997, p. 228), and 1.52 against 1.5 for starch (International Labour Organisation 2004).

DRX analysis of alumina showed no impurities in the commercial powder sample, which was used as received (Fig. 3).

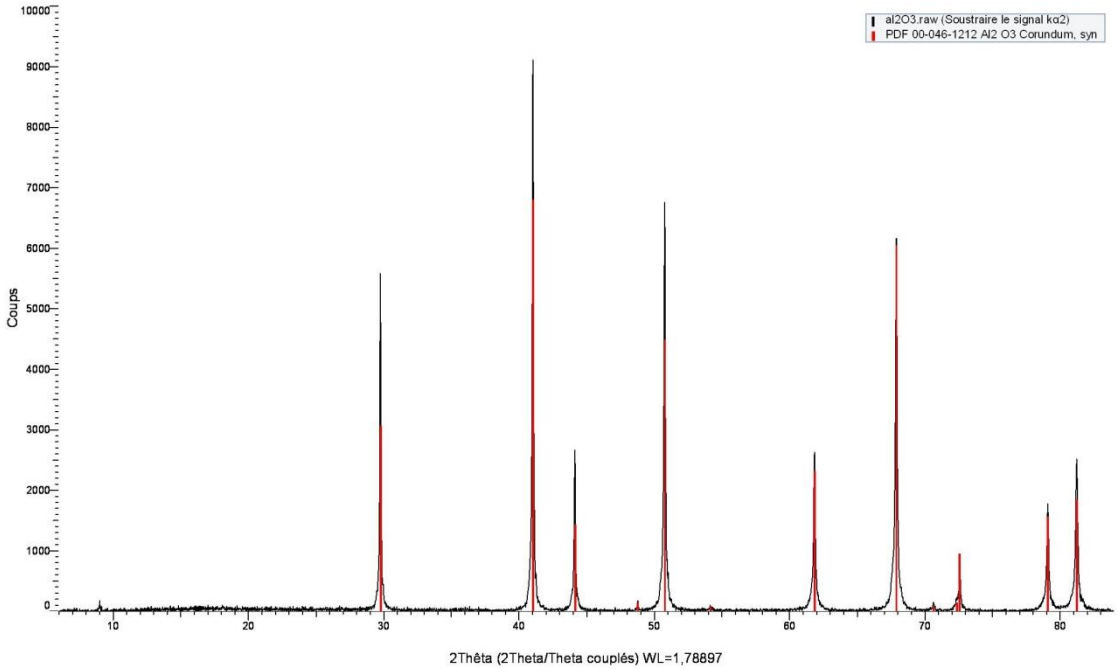


Fig. 3. DRX pattern of alumina powder (corundum).

Table 4. Characteristics of the powders.

Powder	**D50 particle size (µm)**	**BET surface area (m²/g)**	**Density (pycnometry)**
Alumina	1.09	1.64 ± 0.02	3.96
Starch	13.97	0.55 ± 0.02	1.52
Cellulose acetate	218.00	6.73 ± 0.02	1.37

3.2. Rheological measurements

For mixture design purposes, measurements of the complex shear modulus G* were made at 7 min after the beginning of mixing to be close to per-operative conditions. However, it was actually recorded for 10 min, 2 min after the beginning of mixing. Figure 4 shows an example of G', G" and G* curves, depicted against time. In this example, we can note a crossover between the G' and G" curves around 7 min of recording i.e. 9 min after the beginning of mixing. This crossover shows the moment when the material goes from pretty liquid-like (G" > G') to pretty solid-like (G' > G"). Thus, for the precise formulation tested, at 7 min after the beginning of mixing (5 min recording time), the paste is more liquid than solid.

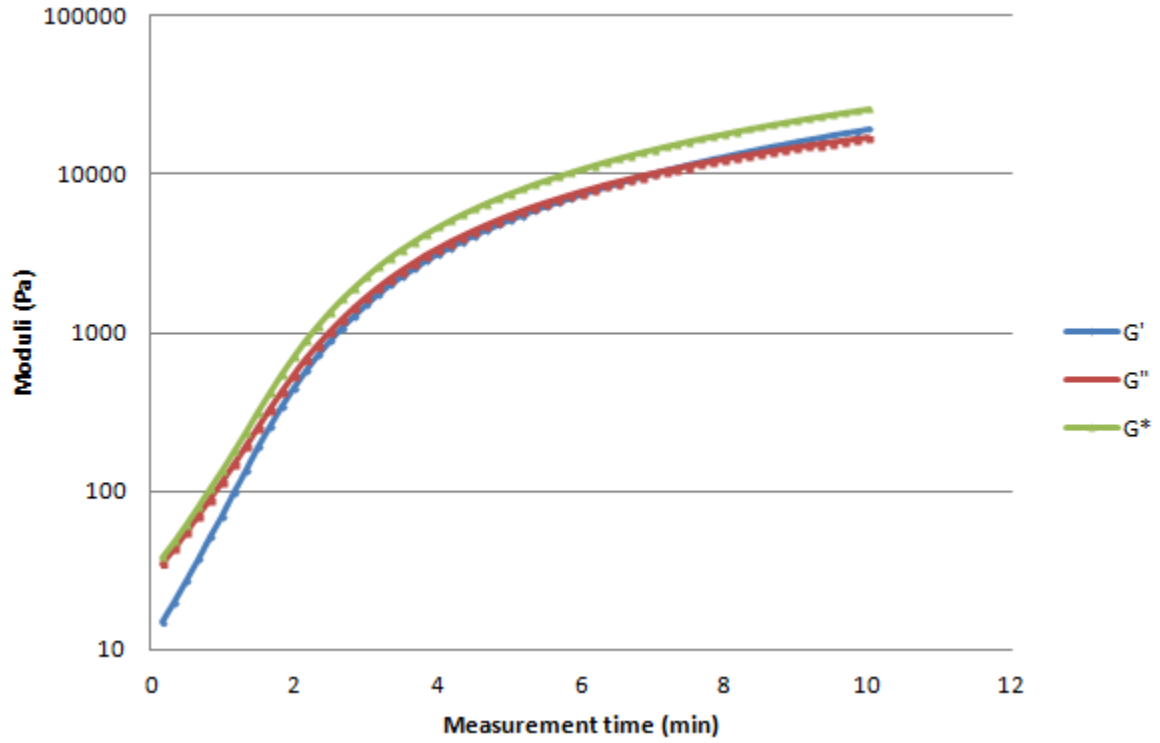


Fig. 4. Elastic (G', blue), viscous (G", red) and complex shear (G*, green) moduli curves, measured for 10 min.

3.3. Mixture design results

3.3.1. Raw data analysis and model evaluation

The viscoelastic properties of the bone cements were represented as a function of time. We chose to measure G* at room temperature at 7 min to be close to per-operative conditions. The results of the experimental campaign are detailed in Table 5.

Table 5. Studied formulations and their measured responses.

Run number	Bioceramic (X_1)	Starch (X_2)	Cellulose acetate (X_3)	G* (Y_{G*}) (Pa)
1	0.75	0.125	0.125	141
2	0.333	0.5	0.167	1,526
3	0.4	0.2	0.4	154,660
4	0.5	0.25	0.25	10,434
5	0.6	0.3	0.1	64
6	0.3	0.4	0.3	73,381
7	0.6	0.1	0.3	26,087
8	0.45	0.45	0.1	89
9	0.41	0.37	0.22	7,022
10	0.63	0.185	0.185	649

11	0.55	0.27	0.18	2,042
12	0.5	0.25	0.25	4,920
13	0.6	0.3	0.1	25
14	0.3	0.4	0.3	96,704
15	0.6	0.1	0.3	31,260
16	0.45	0.45	0.1	129
17	0.5	0.25	0.25	7,549
18	0.6	0.3	0.1	71
19	0.3	0.4	0.3	103,910
20	0.6	0.1	0.3	29,766
21	0.45	0.45	0.1	241

In Table 5, we can see that a very large measuring range is observed for YG response which range from 25 to 154,660 Pa for YG. Prior to the mathematical analysis, a response transform (Box-Cox, Cox 1971) must be achieved whose purpose is: i) to ensure a distribution of responses and consequently of residuals as close to normality as possible, which is recommended in regression data analysis (Montgomery 2001) and ii) to make transformed values of the same order of magnitude otherwise the Lack-Of-Fit test cannot be carried out properly. For our data, the logarithmic function $Z = \log(Y_{G*})$ is the most appropriate response transform to apply. The PLS regression analysis will be completed on Z response values.

The replicate plot of Z responses displayed in Figure 5 shows that the replicate error is low compared to the total response variation, which justifies data modelling to be performed.

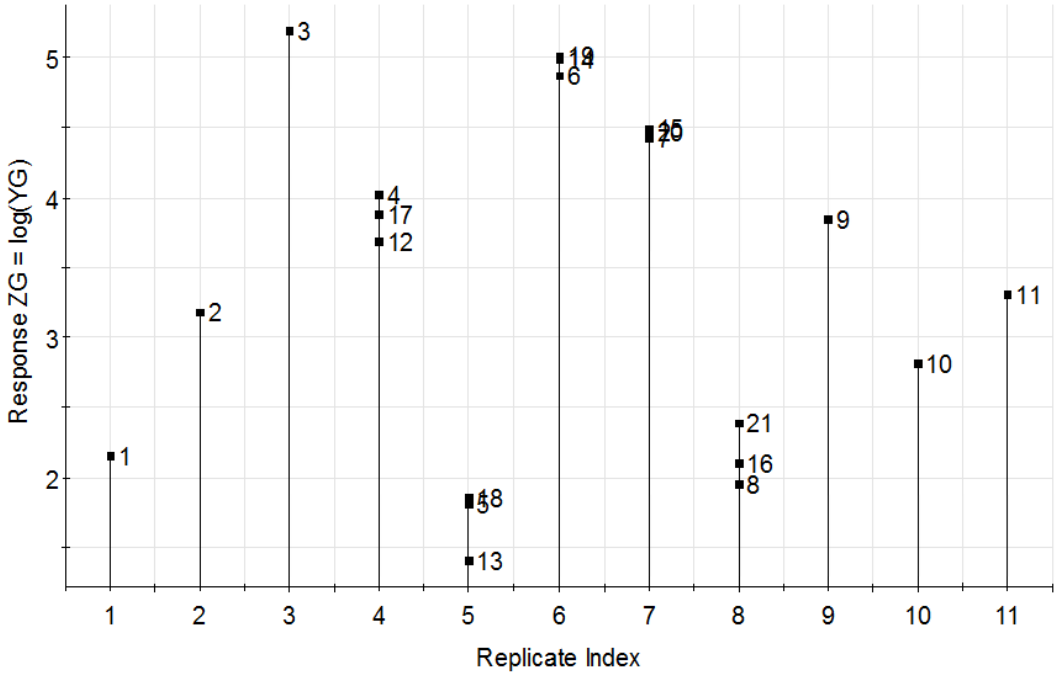


Fig. 5. Replicate plot of the responses $Z = \log(Y_{G*})$.

The PLS analysis on Z values gave model with $R^2 = 0.98$ and $Q^2 = 0.878$ determination coefficients (Table 6). No lack of fit is detectable with $p = 0.124$ which is larger than the reference probability level $p = 0.05$ (Table 6) and residuals are normally distributed with no deviating experiments (Fig. 6). All these features strongly indicate a valid quadratic model.

Table 6. Regression modelling summary of $Z = \log(Y_{G^*})$ data: ANOVA table in which no lack of fit is detectable ($p = 0.124$).

ZG= log(YG)	DF	SS	MS	F	p	SD
			(variance)			
Total	21	276,17	13,151			
Constant	1	245,74	245,736			
Total Corrected	20	30,43	1,52172			1,234
Regression	5	29,82	5,96441	146,11	**0**	2,442
Residual	15	0,612	0,041			0,202
Lack of Fit	5	0,327	0,065	2,291	**0,124**	0,256
(Model Error)						
Pure Error	10	0,285	0,029			0,169
(Replicate Error)						
N = 21	Q2 =	0,878	Cond. no. =	4,919		
DF = 15	R2 =	0,98	Y-miss =	0		
Comp. = 4	R2 Adj. =	0,973	RSD =	0,202		

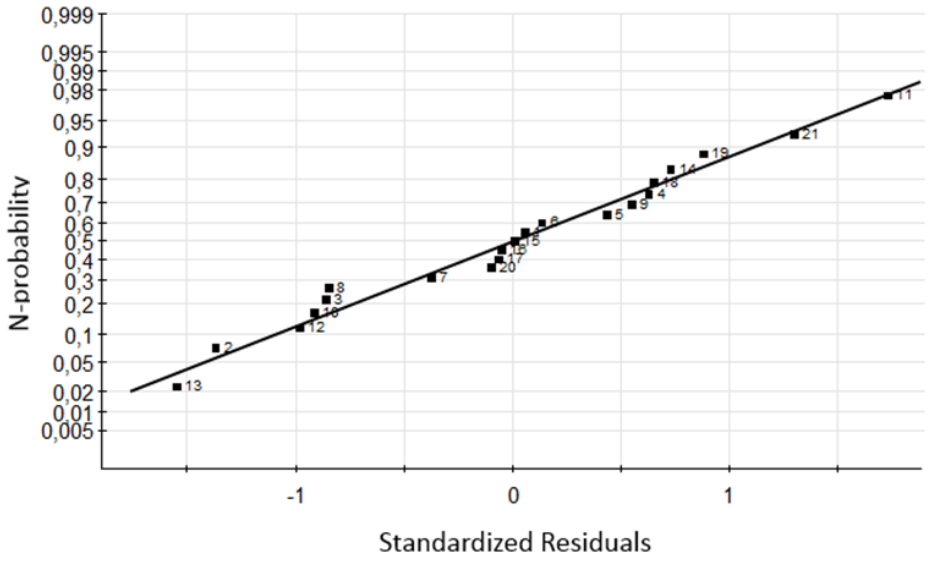


Fig. 6. Regression modelling summary of $Z = \log(Y_{G^*})$ data: Normal probability plot of the response residuals indicating no deviating experiments.

3.3.2. Visualization of the modelling results

Scaled and centered regression coefficients of the computed model are displayed in Figure 7. This coefficient plot mainly shows linear effects of the three mixture factors on the response value Z. Indeed, square and/or interaction terms are small, even though some of them are significant (at 95% confidence level).

The amount of cellulose acetate (X_3) has a major effect on rheological properties. In order to increase the Z value and consequently Y_{G^*} when is applied the inverse response transform $Y_{G^*} = 10^Z$, the amount of cellulose acetate (X_3) should be increased which is a feature already cited in literature (Reis & Cunha 1995), while amounts of both bioceramic (X_1) and corn starch (X_2) must be kept low.

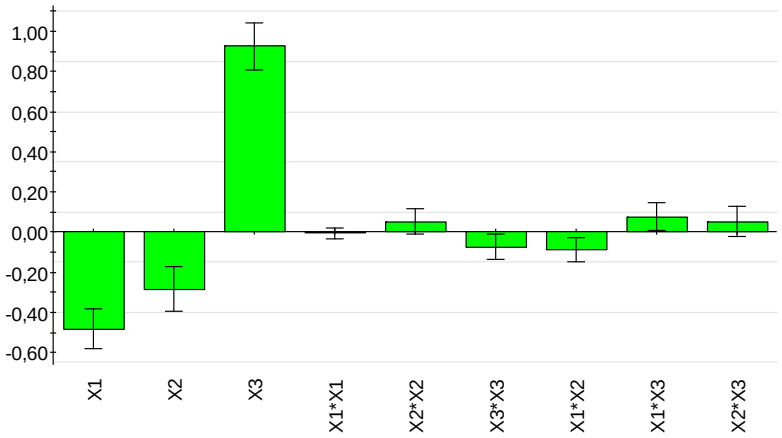


Fig. 7. Coefficient plots for response Z = log(Y_{G*}). We can note the major influence of cellulose acetate (X_3) compared to the bioceramic (X_1) and starch (X_2) on the rheological properties.

In Figure 8 is displayed the mixture contour plot giving Y_{G*} values (in Pa). It is worthwhile noting that the model is capable to cover a very large range in Y_{G*} values from the minimum value 20.3 Pa at point [X_1, X_2, X_3 = 0.75, 0.15, 0.1] to the maximum value 321,000 Pa at point [X_1, X_2, X_3 = 0.3, 0.3, 0.4]. This useful feature enables formulations to be founded in the wide studied experimental domain for many applications. However, this large available range can make the model less accurate. Indeed, we can see from the contour plot (Fig. 8) that small variations of cellulose acetate X_3 proportion cause very fast changes of the predicted Y_{G*} because of the strong effect of X_3 amount (Fig. 7). Consequently, a final adjustment of the mixture factors, and especially X_3, could be required in the validation step.

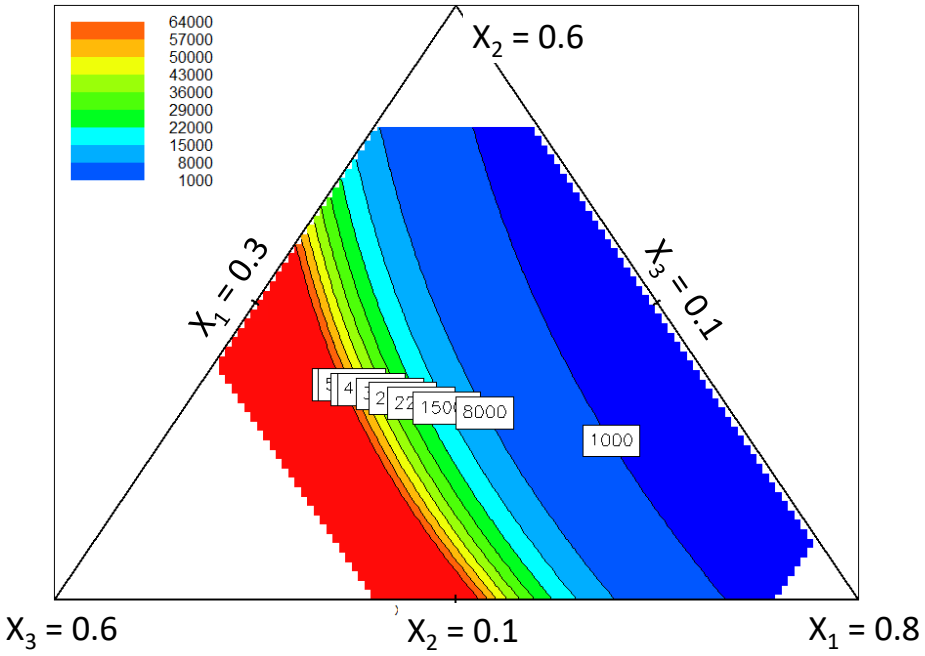


Fig. 8. Mixture contour plot for Y_{G*} response.

The predicted equation derived from the model-fitting procedure is given by Equation 10:

$$Z = 3.432 - 0.485.X_1 - 0.286.X_2 + 0.926.X_3 - 0.076.X_3X_3 - 0.087.X_1X_2 + 0.076.X_1X_3$$

(Eq. 10)

3.3.3. Comparison of the mathematical model versus the experimental tests

No formulation among the 21 runs reported in Table 5 gave an experimental Y_{G*} close enough to targeted values. That is why the mixture design is a must to optimize the formulation of our cements.

The characteristics of the desired formulations developed in our study are summarized as follows: i) G* response value must be as close as possible to the G* of the commercial cements (similar $G^*_{Palacos}$, similar $G^*_{Simplex}$, similar G^*_{Zimmer}), and ii) the amount of bioceramic X_1 must be as high as possible.

As shown from the contour plot (Fig. 8), whatever the selected value of Y_{G*}, these conditions were always fulfilled with a formulation where X_2 is kept at its lowest value, i.e. X_2 = 0.1. By using the model given by Equation 10, we have then simply adjusted the X_3 proportion the final formulations predicted by the model to aim at the three chosen target values shown in Table 7. This X_3 adjustment was carried out up to a maximum of three decimal places, which explains why the target and predicted values do not perfectly match.

Table 7. Predictive formulations for the rheological response Y developed for the target G* values.

Exp. No.	Bioceramic (X_1)	Starch (X_2)	Cellulose acetate (X_3)	Target values G^*_{target} (Pa)	Predicted values G^*_{mod} (Pa)
Similar $G^*_{Palacos}$	0,563	0.1	0,337	57025	**56844**
Similar $G^*_{Simplex}$	0,591	0.1	0,309	33155	**33138**
Similar G^*_{Zimmer}	0,731	0.1	0,169	725	**725**

The three "similar G^*_{XX}" points were tested experimentally and the measurement was repeated four times. Results are reported in Table 8.

Table 8. Results of optimized formulations.

	Similar $G^*_{Palacos}$	Similar $G^*_{Simplex}$	Similar G^*_{Zimmer}
X3 proportion	0.337	0.309	0.169
Predicted values (Pa)	**56,844**	**33,138**	**725**
# 1 (Pa)	63,411	43,998	1,528.0
# 2 (Pa)	59,347	45,611	957.5
# 3 (Pa)	59,694	39,051	814.0
# 4 (Pa)	50,701	47,340	1,802.3
Mean value (Pa)	**58,288**	**44,000**	**1,275**
95 % Confidence Interval (±) (Pa)	8,564	5,681	744

The results presented in Table 8 suggest the following analysis: the confidence interval ranges from 49,724 to 66,853 Pa for the similar $G^*_{Palacos}$. The predicted value (56,844 Pa) belongs to that interval, showing the performance of the model. The same observations can be proposed when applying the model to the similar G^*_{Zimmer}: the confidence interval goes from 532 to 2,019 Pa, which includes the predicted value of 725 Pa. For these two formulations, the developed mathematical model is experimentally validated and therefore predicts well.

For the similar $G^*_{Simplex}$, the mean experimental value is outside the confidence interval and slightly exceeds the predicted value. However, given the wide range of variation of G*, the positive point is that our mathematical model is able to predict a value which has the correct order of magnitude as the experimental values. Nevertheless, a final adjustment of proportions is required and our attention was focused on X_3 proportion. Indeed, as discussed above and shown in the contour plot (Fig. 8), the value of G* may vary significantly even for very small variations of X_3, particularly where X_3 ranges between 0.3 and 0.4.

Adjustment of X_3 amount may be easily performed by considering points 7, 15 and 20 from the initial mixture design at [X_1, X_2, X_3 = 0.6, 0.1, 0.3] and the similar $G^*_{Simplex}$ points (points B) repeated four times at [X_1, X_2, X_3 = 0.591, 0.1, 0.309] (Table 9). These seven points were all measured with the same X_2 proportion: X_2 = 0.1. Thus X_3 proportion is the single adjustable parameter since X_1 is constrained by the external constraint $X_1 + X_2 + X_3 = 1$.

Table 9. X_3, Y_{G^*} and Z values of points 7, 15 and 20 from the initial design and of points B from the similar $G^*_{Simplex}$ runs.

Run	Cellulose acetate (X_3)	G* (Y_{G^*}) (Pa)	Z = log (Y_{G^*})
Point B run No.1	0.309	43,998	4.6434
Point B run No.2	0.309	45,611	4.6591
Point B run No.3	0.309	39,051	4.5916
Point B run No.4	0.309	47,340	4.6752
Exp. No. 7	0.300	26,087	4.4164
Exp. No. 15	0.300	31,260	4.4950
Exp. No. 20	0.300	29,766	4.4737

The logarithmic response transform as already used in Section 3.3.1 was applied to Y_G responses reported in Table 9 and linear regression was subsequently applied to Z data (Fig. 9). Use of the regression equation shows that for X_3 = 0.303, the predicted Y_{G^*} is equal to 33,259 Pa, that is very close to the target value (similar $G^*_{Simplex}$ =33,138 Pa). So, for the similar $G^*_{Simplex}$, the cellulose acetate amount needs to be modified with a variation of 2% only of initial X_3 proportion predicted by the mathematical model to achieve the objective in terms of G*.

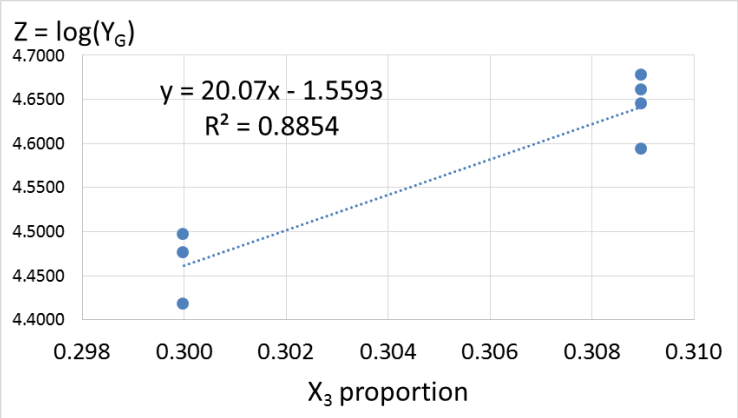


Fig. 9. Graph of Z values as a function of X_3 proportion for experiments given in Table 9 and linear regression equation.

The objective of the study was to obtain a mathematical model which could adapt to any G* required for specific cement uses of the surgeon: may it be as a dough to tighten the adhesion between bone and prosthesis, or as an injectable paste to fill in bone cavities or in dental applications. This objective is largely achieved with a mathematical model built up from the mixture design which is working well overall, even though final proportion adjustments may be necessary to be carried out. This study shows the power of DoE to extract information hidden in datasets, allowing us to optimize formulations of materials according to target values linked to their final use, as well as to understand phenomena driven by the effect of all the components of the material.

4. CONCLUSIONS

The rheological properties and especially the determination of the complex shear modulus G* are crucial for the development of bone cements. From a new composite cement containing cellulose acetate, starch, a bioceramic and an acrylic hydrogel, formulations with different G* were made in order to adapt to various clinical applications.

The DoE tool did show its importance in this work and allowed us, inter alia, to underline the effect of the factors and the correlation between cellulose acetate amount and G*.

Thanks to this work, by applying the DoE method and implementing a mixture design, the formulation of a cement with a cellulose acetate/starch/alumina matrix will be easily and quickly adjusted to a considered clinical application.

REFERENCES

Aho, J, Boetker, JP, Baldursdottir, S &Rantanen, J 2015, 'Rheology as a tool for evaluation of melt processability of innovative dosage forms', *International Journal of Pharmaceutics*, vol. 494, pp. 623-642.

Boesel, LF, Mano, JF & Reis, RL 2004, 'Optimization of the formulation and mechanical properties of starch based partially degradable bone cements', *Journal of Materials Science: Materials in Medicine*, vol. 15, pp. 73-83.

Boesel, LF & Reis, RL 2004, 'Hydrophilic matrices to be used as bioactive and degradable bone cements', *Journal of Materials Science: Materials in Medicine*, vol. 15, pp. 503-506.

Boesel, LF, Cachinho, SCP, Fernandes, MHV &Reis, RL 2007,'The in vitro bioactivity of two novel hydrophilic, partially degradable bone cements', *ActaBiomaterialia*, vol. 3, pp. 175–182.

Bohner, M 2000, 'Calcium orthophosphates in medicine: from ceramics to calcium phosphate cements', *Injury*, vol. 31, pp. D37-D47.

Buchbinder, R, Golmohammadi, K, Johnston, RV, Owen, RJ, Homik, J, Jones, A, Dhillon, SS, Kallmes, DF & Lambert, RGW 2015, 'Percutaneous vertebroplasty for osteoporotic vertebral compression fracture', *The Cochrane Library*.

Chaudhry, S & Dunlop, D 2012, 'Bone cement in arthroplasty', *Orthopaedics and Trauma*, vol. 26, pp. 391-396.

Combes, C, Tadier, S, Galliard, H, Girod-Fullana, S, Charvillat, C, Rey, C, Auzély-Velty, R & El Kissi, N 2010, 'Rheological properties of calcium carbonate self-setting injectable paste', *Acta Biomaterialia*, vol. 6, pp. 920-927.

Cox, DR 1971, 'A note on polynomial response functions for mixtures', *Biometrica*, vol. 58, pp. 155-159.

Dorozhkin, SV 2010, 'Bioceramics of calcium orthophosphates', *Biomaterials*, vol. 31, pp. 1465-1485.

Eliaz, N &Metoki, N 2017, 'Calcium phosphate bioceramics: a review of their history, structure, properties, coating technologies and biomedical applications', *Materials*, vol. 10, pp. 334.

Eriksson, L, Johansson, E, Kettaneh-Wold, N, Wikstroem, C & Wold, S 2008, *Design of experiments: principles and applications*, 3rdedn, Umetrics, Umeå.

Farrar, DF & Rose J 2001, 'Rheological properties of PMMA bone cements during curing', *Biomaterials*, vol. 22, pp. 3005-3013.

Greenberg, AR &Kamel, I 1976, 'Polymer-ceramic composite for tooth-root implant', *Journal of Biomedical Materials Research Part A*, vol. 10, pp. 777-788.

Guo, D, Xu, K, Zhao, X & Han, Y 2005, 'Development of a strontium-containing hydroxyapatite bone cement', *Biomaterials*, vol. 26, pp. 4073-4083.

International Labour Organization 2004, *Starch ICSC: 1553*, International Chemical Safety Cards, International Programme on Chemical Safety, viewed 19 May 2017, <http://www.ilo.org/dyn/icsc/showcard.display?p_card_id=1553>

Kettaneh-Wold, N 1992, 'Analysis of mixture data with partial least squares', *Chemometrics and Intelligent Laboratory Systems*, vol. 14, pp. 57-69.

Lewis, G 1997, 'Properties of acrylic bone cement: State of the art review', *Journal of Biomedical Materials Research Part B: Applied Biomaterials*, vol. 38, pp. 155-182.

Lewis, RJ Sr (ed.) 1997, *Hawley's Condensed Chemical Dictionary*,13thedn, John Wiley & Sons Inc., New York.

Lewis, RJ Sr (ed.) 2007, *Hawley's Condensed Chemical Dictionary*,15thedn, John Wiley & Sons Inc., New York.

Marrs, B, Andrews, R, Rantell, T & Pienkowski, D 2006, 'Augmentation of acrylic bone cement with multiwall carbon nanotubes', *Journal of Biomedical Materials Research Part A*, vol. 77, pp. 269-276.

Montgomery, DC 2001, *Response surface methods and other approaches to process optimization. Design and analysis of experiments*, Wiley, New York.

Pereira, CS, Cunha, AM, Reis, RL, Vázquez, B & San Román, J 1998, 'New starch-based thermoplastic hydrogels for use as bone cements or drug-delivery carriers', *Journal of Materials Science: Materials in Medicine*, vol. 9, pp. 825-833.

Reis, RL & Cunha, AM 1995, 'Characterization of two biodegradable polymers of potential application within the biomaterials field', *Journal of Materials Science: Materials in Medicine*, vol. 6, pp. 786-792.

Saha, S & Pal, S 1984, 'Mechanical properties of bone cement: a review', *Journal of Biomedical Materials Research*, vol. 18, pp. 435-462.

Van Wazer, JR, Lyons, JW, Kim, KY & Colwell, RE 1963, *Viscosity and flow measurement: a laboratory handbook of rheology*, Interscience Publishers, New York-London.

Wold, S, Ruhe, A, Wold, H & Dunn, WJ III 1984, 'The collinearity problem in linear regression. The partial least squares approach to generalized inverses', *SIAM Journal on Scientific and Statistical Computing*, vol. 5, pp. 735-743.